N94- 30617

209924

P- 30

Atmosphere, Ocean, and Land: Critical Gaps in Earth System Models

Ronald G. Prinn and Dana Hartley

Introduction

The earth's unique environment for life is determined by an interactive system comprising the atmosphere, ocean, land, and the living organisms themselves. We know from observations that this system is not static but changing. Our ability to understand past changes and predict future changes is hampered by insufficient understanding of at least five fundamental processes in the earth system: (1) convection, condensation nuclei, and cloud formation; (2) oceanic circulation and its coupling to the atmosphere and cryosphere; (3) land surface hydrology and hydrology-vegetation coupling; (4) biogeochemistry of greenhouse gases; and (5) upper atmospheric chemistry and circulation.

We need to improve our knowledge of each of these processes through a combination of observations and theory (model development). We then need to incorporate realistic models for these processes into climate prediction models with special attention to potential feedbacks to climate change involving these processes (Figure 1). In each case it is not just a matter of explaining the present state but also of understanding how each of the processes contributing to this state will change when one or more of the external forcing mechanisms changes. In this paper we briefly review current knowledge and pinpoint some of the major areas of uncertainty for each of the above five fundamental processes.

Convection, Condensation Nuclei, and Cloud Formation

Clouds and water vapor play a major role in the heat budget of the earth's surface. Clouds contribute to surface cooling by reflect-

ing sunlight back to space. In fact, cloud albedo doubles the albedo of the entire earth over what it would be in the absence of clouds (Ramanathan et al., 1989). Furthermore, both water vapor and clouds contribute to surface heating by absorbing and re-emitting infrared radiation (greenhouse effect). Indeed, the contribution to
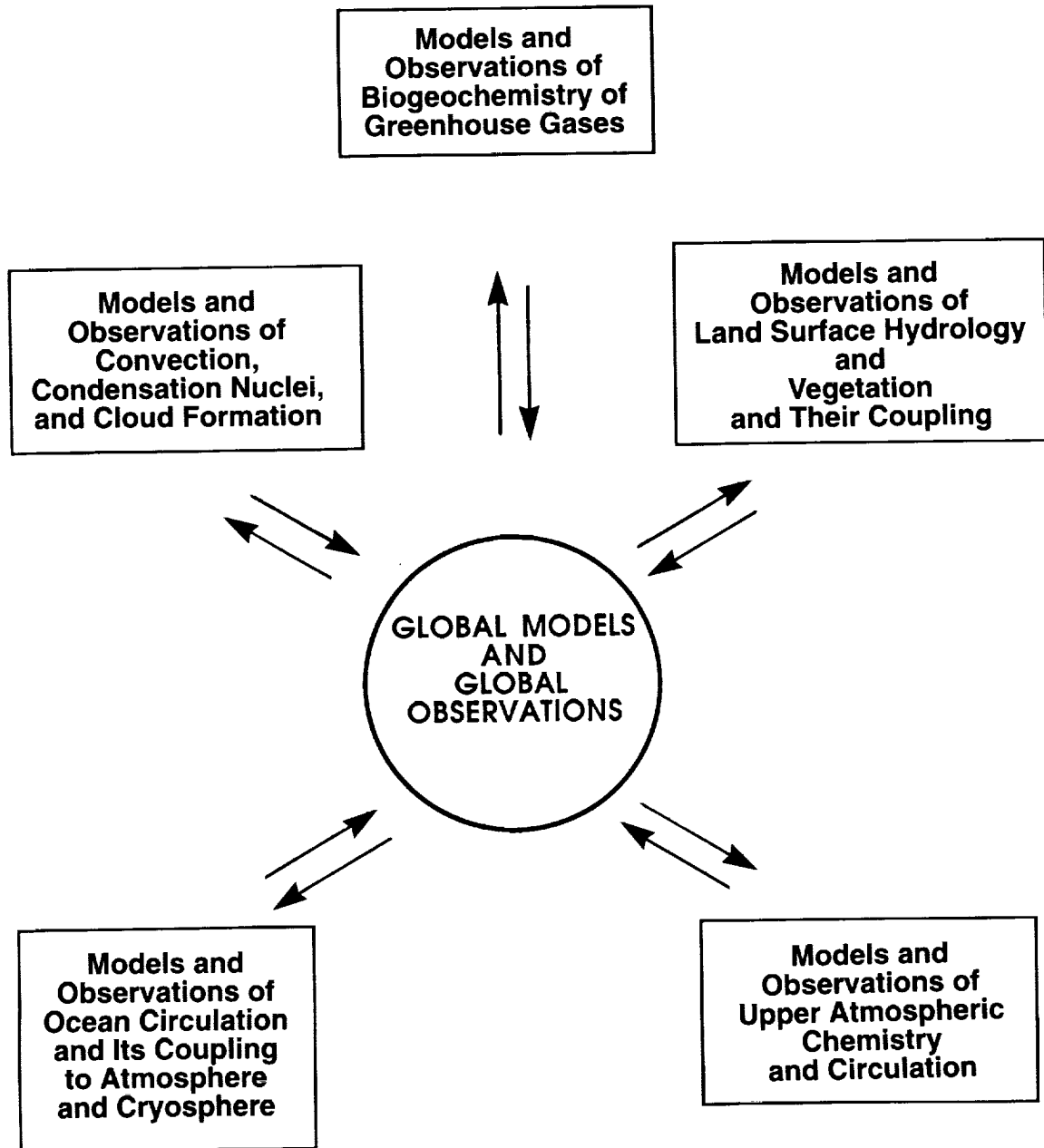
```
┌─────────────────────┐
│   Models and        │
│   Observations of   │
│   Biogeochemistry of│
│   Greenhouse Gases  │
└─────────────────────┘

┌─────────────────────┐              ┌─────────────────────┐
│   Models and        │      ↑  │    │   Models and        │
│   Observations of   │      │  │    │   Observations of   │
│   Convection,       │      │  ↓    │   Land Surface      │
│   Condensation      │             │   Hydrology and     │
│   Nuclei, and       │             │   Vegetation and    │
│   Cloud Formation   │             │   Their Coupling    │
└─────────────────────┘             └─────────────────────┘

              ╱    GLOBAL MODELS   ╲
                    AND
                    GLOBAL
                    OBSERVATIONS

┌─────────────────────┐             ┌─────────────────────┐
│   Models and        │             │   Models and        │
│   Observations of   │             │   Observations of   │
│   Ocean Circulation │             │   Upper Atmospheric │
│   and Its Coupling  │             │   Chemistry         │
│   to Atmosphere     │             │   and Circulation   │
│   and Cryosphere    │             │                     │
└─────────────────────┘             └─────────────────────┘
```

Figure 1. Schematic illustrating required research for improving current climate models.

the greenhouse effect of clouds and water vapor is far greater than that caused by CO_2 (see Table 1 for chemical names and formuli) and the other long-lived greenhouse gases.

Table 1: Chemicals named in this chapter

^{12}C	carbon-12
^{13}C	carbon-13
$CFCL_3$	trichlorofluoromethane (CFC-11)
CF_2Cl_2	dichloro-difluoromethane (CFC-12)
$CF_2ClCFCl_2$	1-chlorodifluoro-2-dichlorofluoroethane (CFC-113)
$CHClF_2$	chlorodifluoromethane (HCFC-22)
$CHCl_2CF_3$	1-dichloro-2-trifluoroethane (HCFC-123)
CH_2FCF_3	1-trifluoro-2-fluoroethane (HCFC-134a)
CH_3CCl_3	1-trichloroethane (methyl chloroform)
CH_35Cl_3 (DMS)	dimethyl sulfide
CH_4	methane
Cl	chlorine atom
ClO	chlorine monoxide
$ClONO_2$	chlorine nitrate
ClOOCl	chlorine monoxide dimer
Cl_2	molecular chlorine
CO	carbon monoxide
CO_2	carbon dioxide
HCl	hydrogen chloride
HNO_3	nitric acid
HO_2	hydroperoxyl free radical
H_2O	water
H_2O_2	hydrogen peroxide
NO	nitric oxide
NO_2	nitrogen dioxide
N_2O	nitrous oxide
$O(^1D)$	electronically excited oxygen atom
OH	hydroxyl free radical
O_2	molecular oxygen
O_3	ozone
RH	generic hydrocarbon
RO_2	generic organic peroxy free radical
ROOH	generic organic hydroperoxide
SO_2	sulfur dioxide

The net effect of clouds is determined by the opposing effect of the albedo of the cloud and its opacity to infrared radiation. Theory and observations have shown that the net effect of clouds is to lower the surface temperature relative to the cloud-free state (Somerville and Remer, 1984; Ramanathan et al., 1989). However, there are still difficulties in representing the present cloud forcing in large-scale general circulation models (GCMs). A recent comparison between GCM results and present-day observations illustrates some of the weaknesses in present parameterizations of cloud formation (Kiehl and Ramanathan, 1990). Figure 2 in particular shows that there is too much solar radiance reaching the surface near the poles and too little near the tropics in the community climate model (CCM) of the
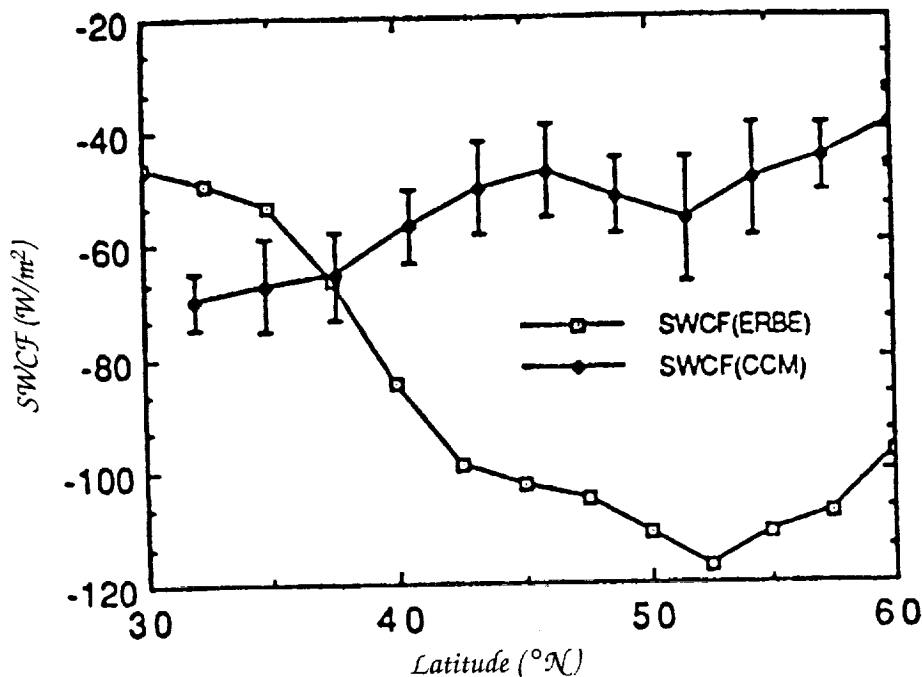
Figure 2. *Shortwave cloud radiative forcing (SWCF) as a function of latitude in the western North Atlantic from ERBE data and from the NCAR community climate model (adapted from Kiehl and Ramanathan, 1990).*

National Center for Atmospheric Research as compared to Earth Radiation Budget Experiment (ERBE) data. Some of this difference is associated with the surface albedo's being too large in the model tropics and some with obvious gaps in the ability of the CCM to parameterize the cloud formation process. Furthermore, for predictions of future climate change, we want to be capable of determining how the cloud/radiative balance may change, which requires a fundamental understanding of the cloud formation process. We then need realistic models for linking cloud microphysics and atmospheric dynamics to yield accurate predictions of the global three-dimensional structure of clouds.

The microphysics of clouds is determined to a large extent by the ambient concentrations of cloud condensation nuclei (CCN). Over land the presence of CCN is often due to dust or aerosol emissions by humans. Over the oceans the predominant source of CCN is either land-derived CCN and CCN precursors like SO_2 advected off the land, or the CCN precursor dimethyl sulfide (DMS), which is produced in the surface ocean itself by planktonic algae (see, e.g., Charlson et al., 1987). The more CCN available, the smaller the cloud

droplets will be. Twomey (1977) demonstrates in addition that for a fixed volume of cloud water, the smaller the particles, the greater the albedo. Charlson et al. (1987) have specifically calculated (Figure 3) the change in cloud-top albedo as compared to a reference cloud as the droplets either grow or become smaller with the same total liquid water content. The top axis in Figure 3 indicates how this change is related to the number of droplets. Thus, as the number of droplets
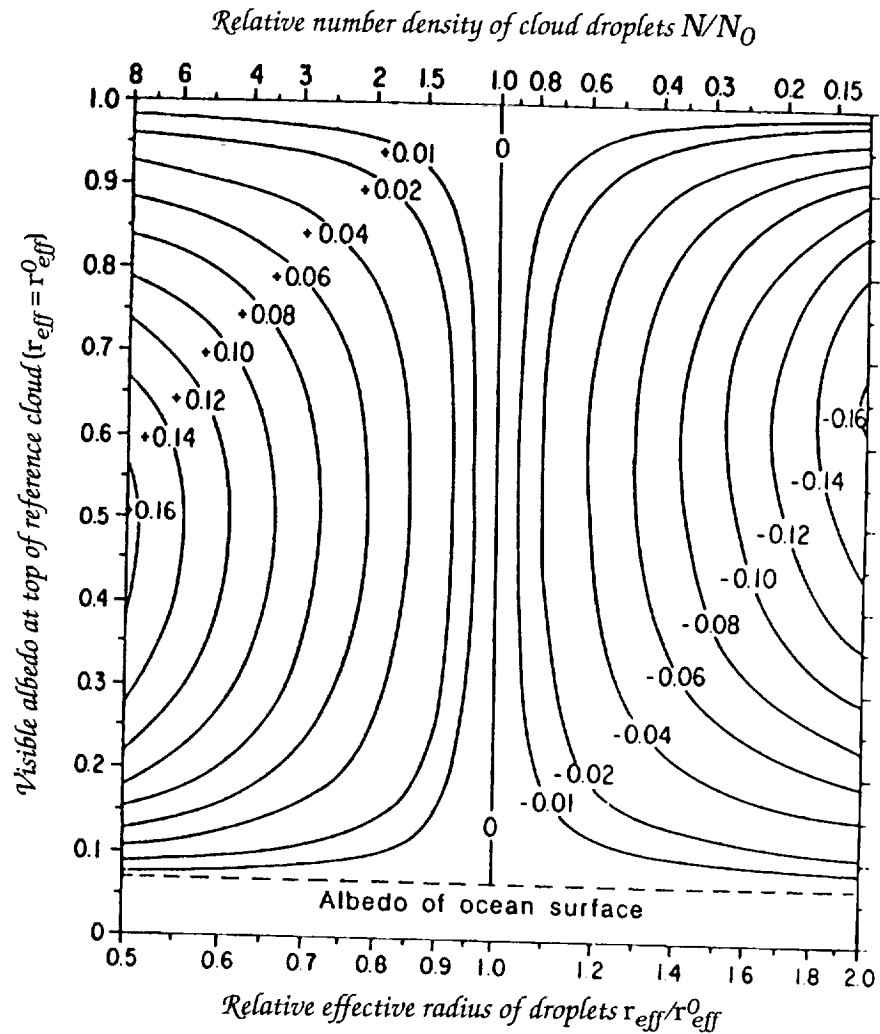

Figure 3. Contours showing change of visible albedo caused by changing droplet number density N or equivalently droplet effective radius r_{eff} relative to a reference cloud (N_0, r^0_{eff}). Albedo at top of reference cloud given on left-hand vertical scale (adapted from Charlson et al., 1987; reprinted by permission from Nature, © 1987 Macmillan Magazines Ltd.).

increases, as would be the case if more CCN were available due to increased DMS emissions, the albedo increases. Therefore, any climate changes that influence the emissions of DMS over the oceans may induce a cloud-climate feedback associated with them. Understanding how CCN may change is therefore an important aspect of predicting future cloud cover and rainfall.

The three-dimensional structure of optically thick clouds is important. For very deep clouds, the downward emission from the warm cloud base significantly exceeds the upward emission from the cool cloud top. Very shallow clouds, on the other hand, exhibit much smaller differences between these fluxes, so the greenhouse effect due to them is much smaller. This influences the competition between the albedo and greenhouse effect of clouds. For example, Ramanathan and Collins (1991) have recently argued that relatively thin, highly reflective cirrus clouds formed during El Niño may effectively limit the magnitude of the sea surface temperature increase being forced by the greenhouse effect of water vapor and clouds. The three-dimensional structure of clouds depends on both mesoscale processes (convection) and the larger-scale circulation and is poorly predicted in current climate models.

Convection also has a large influence on the surface heat budget. Evaporation and subsequent convection serve to cool and dry the surface and lower troposphere. In turn, the middle and upper troposphere are warmed by condensation. The distribution of water vapor and also many chemically important trace species is strongly influenced by convection and its subsequent motions. As shown by Dickerson et al. (1987), the convective motions tend to transport tracers from the lower troposphere to upper levels. Figure 4 illustrates the redistribution of carbon monoxide. To the left of the cloud the normal vertical distribution is evident, with the CO mixing ratio decreasing with height. However, within the cloud, the situation has reversed as the high-CO air in the boundary layer has been transported to the upper troposphere, leaving the lower levels depleted in CO relative to the normal situation.

For climate prediction models we clearly need realistic models for convection, including its roles in heat, momentum, and trace species (e.g., water vapor) transport, and in cloud formation. The first step in developing a cloud model is to understand the basic processes, and the second step is to parameterize these processes for inclusion in GCMs, in which they are subgrid-scale phenomena. Previous attempts at producing convective parameterizations have had their drawbacks. For example, Manabe et al. (1965) used a straightforward convective adjustment scheme that adjusts the atmospheric lapse rate back to an observed neutral state for satu-
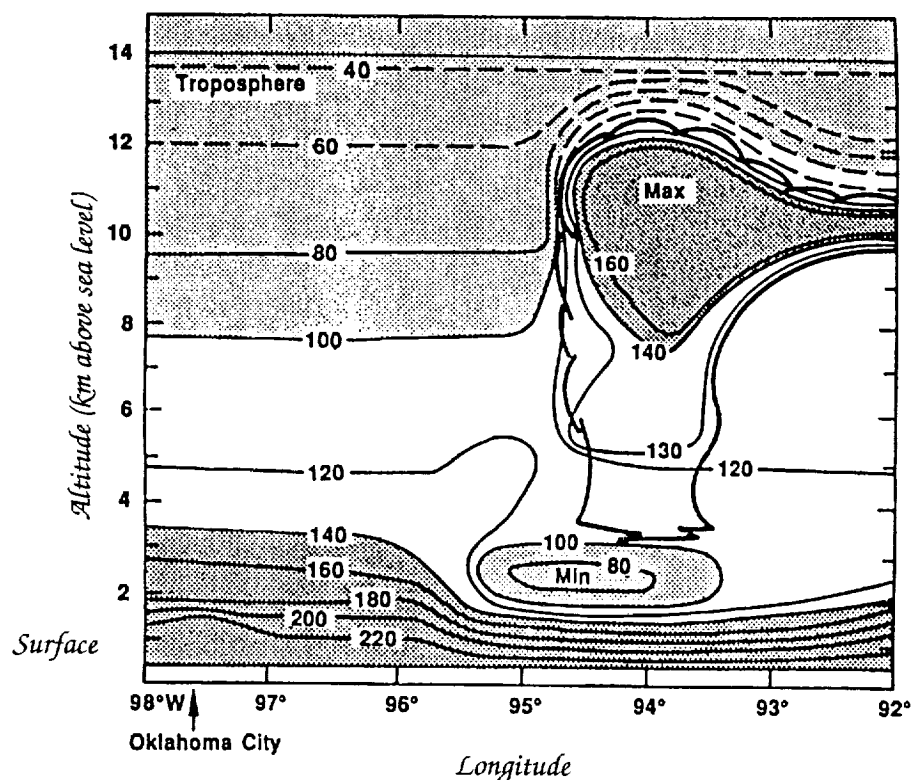
Figure 4. Concentration of carbon monoxide (ppbv) as a function of altitude
and latitude over Oklahoma City, Oklahoma, both outside and within a
thunderstorm (adapted from Dickerson et al., 1987; © 1987 by the AAAS).

rated regions. Unfortunately, this means instability can build up in
unsaturated regions. A recent parameterization by Betts (1986)
allows for adjustment in unsaturated regions, but it still does not
predict the profiles of temperature or water vapor. Instead, these are
adjusted to observed profiles. Emanuel (1990) allows for the predic-
tion of water vapor content but relies on a specified vertical distribu-
tion of precipitation. The major drawback of the above schemes is
that they are all based on adjusting the atmosphere back to an
observed structure. For purposes of climate change models, this
type of parameterization is quite suspect since certain potentially
important climate changes are omitted. The Kuo (1974) scheme is
more physical. In this scheme convection occurs when there is
moisture convergence. However, this also has its problems. Regions
can get extremely unstable, yet unless there is a transport of mois-
ture into that region, no convection occurs. Realistic models for con-
vection and cloud formation are clearly an important requirement
for GCMs to be used for future climate change predictions.

Oceanic Circulation and Its Coupling to the Atmosphere and Cryosphere

The oceanic circulation has major influences on the climate system. In the energy balance of the earth, the ocean circulation is important in the heat transport from equator to pole. Figure 5 shows the heat transport for both the oceans and the atmosphere as determined by Carissimo et al. (1985) and earlier workers. The oceanic and atmospheric heat transport have comparable strengths. Thus, it is evident that the ocean is crucial to consider and without it the latitudinal temperature gradient would probably be significantly larger. The ocean circulation also contributes to the determination in space and time of the latent, sensible, and radiative heating of the troposphere. For studying possible climate changes, the changes in water vapor input from the ocean with changing sea surface temperature are a critical feedback (Ramanathan, 1981). Another way the ocean circulation affects the heating in the troposphere is in its interaction with sea ice. Figure 6 gives some results from Hibler (1990) and earlier papers which show how important it is to consider the ice dynamics. There is about 50% more ice when there is no ice dynamics. The greater the extent of the sea ice, the more it can decrease the heat flux between the ocean and the atmosphere (Bentley, 1984). Since generally, in the polar regions, the ocean is warmer than the atmosphere, the extent of sea ice can greatly influence the temperature of the tropospheric air. Furthermore, the albedo of sea ice is about 0.9 whereas that of sea water is about 0.1. Thus, the radiative heating of the troposphere is influenced by sea ice cover, which in turn is affected by the ocean circulation.

The ocean circulation is essential for transporting nutrients to the surface of the open oceans in order to feed phytoplankton and other marine organisms (Broecker and Peng, 1982). An example of the importance of this process is seen during an El Niño year when the usual East Pacific equatorial upwelling is suppressed. As a consequence there are no new nutrients, and the fish die off, which is devastating for the Peruvian fishing industry (Philander and Rasmusson, 1985).

Finally, the ocean serves as a sink for thermal energy and carbon dioxide as they increase in the atmosphere. The ability of the ocean to do this depends greatly on the strength of its circulation. Figure 7 is a result from Hansen et al. (1985) showing the different temperature increases expected with different vertical diffusion rates in a highly simplified ocean model. Obviously, the ocean serves as a large heat sink since its heat capacity is so much greater than the atmosphere's, but its ability to do so depends on its circulation. This is also true in the uptake of CO_2. Siegenthaler (1983) explored the effects of circulation on the uptake of CO_2, and one of his results is shown in Figure 8 which illustrates how much more CO_2 is taken
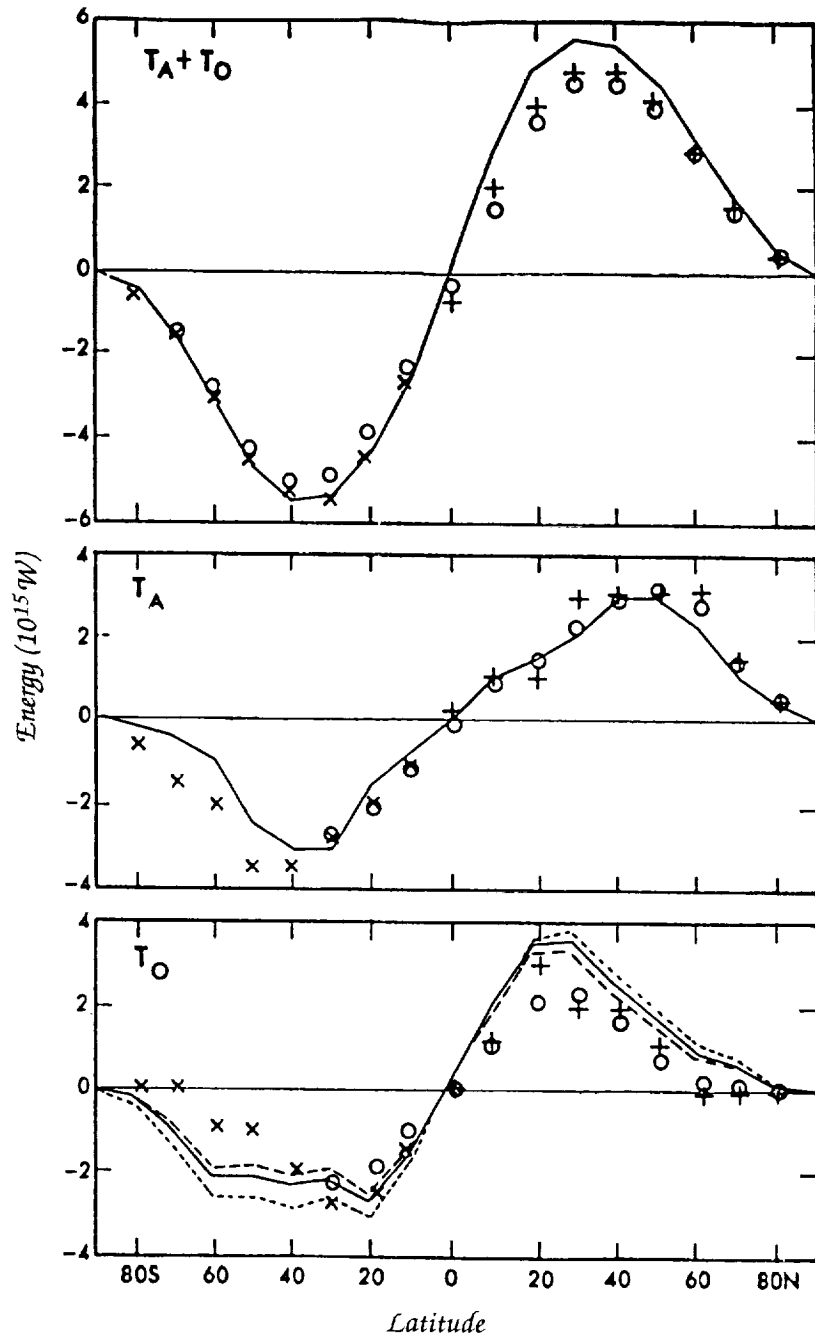
Figure 5. Annual meridional transport of energy $(10^{15}$ W) in the atmosphere plus ocean $(T_A + T_O)$, atmosphere (T_A), and ocean (T_O) computed by Carissimo et al. (1985) and compared to previous investigators: (+) Oort and Vonder Haar, 1976; (x) Trenberth, 1979; (O) Newell et al., 1972 (adapted from Carissimo et al., 1985; © American Meteorological Society).
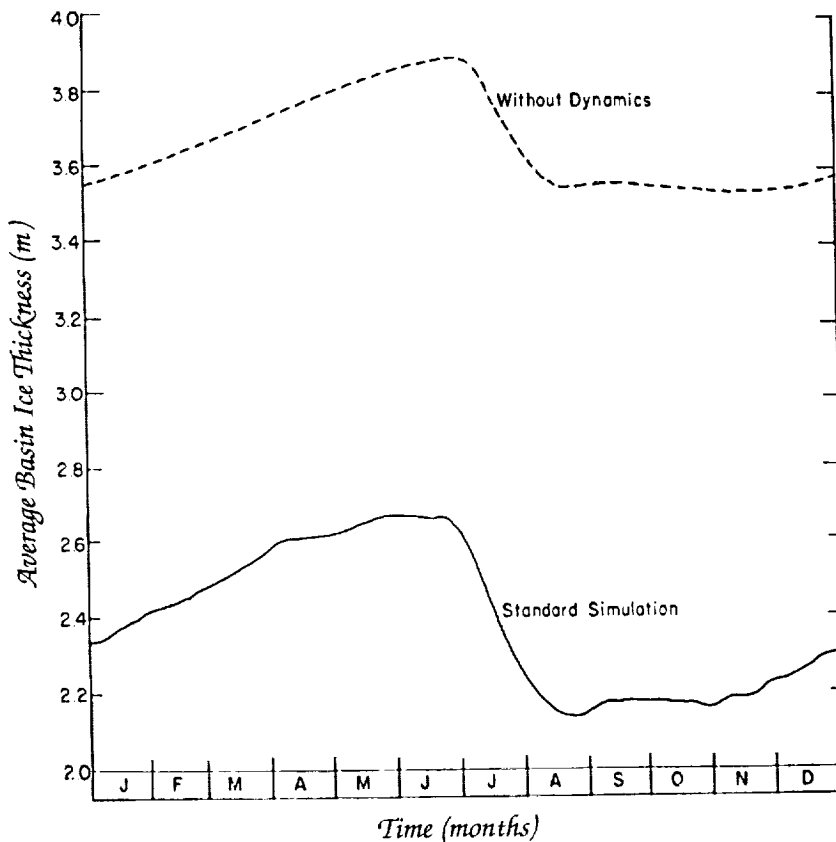
Figure 6. Comparison of Arctic basin average ice thickness (m) for a two-level model without dynamics and with dynamics (standard) (adapted from Hibler, 1990; © American Meteorological Society).

into the ocean when there is efficient downward advection in "outcrop" regions like the Norwegian and Weddell seas.

The atmosphere also influences the ocean since the upper ocean circulation is forced by atmospheric winds. This coupling is exemplified by the El Niño/Southern Oscillation (ENSO) phenomenon, during which the warming of the eastern equatorial Pacific is accompanied by slowing of the trade winds and by an eastward extension of the western Pacific convection zone. Slowing of the trade winds decreases the upwelling associated with Ekman drift, thus contributing to the warming of the eastern Pacific. The assignment of cause and effect in this coupled ocean-atmosphere phenomenon is difficult to make (Philander and Rasmusson, 1985).

The ocean circulation and sea ice are also coupled. When ice is formed, the ocean becomes more saline, tending to increase the

oceanic overturning (Hibler, 1990). If the ice is transported by the combined effects of the winds and the ocean circulation (which are related) and then melts in another region, this latter region becomes less saline, and overturning is inhibited there. One possible consequence of this could be changes in the northern Atlantic climate. The Gulf Stream transports warmer water northward. When it reaches the North Atlantic the water cools, thereby warming the tro-
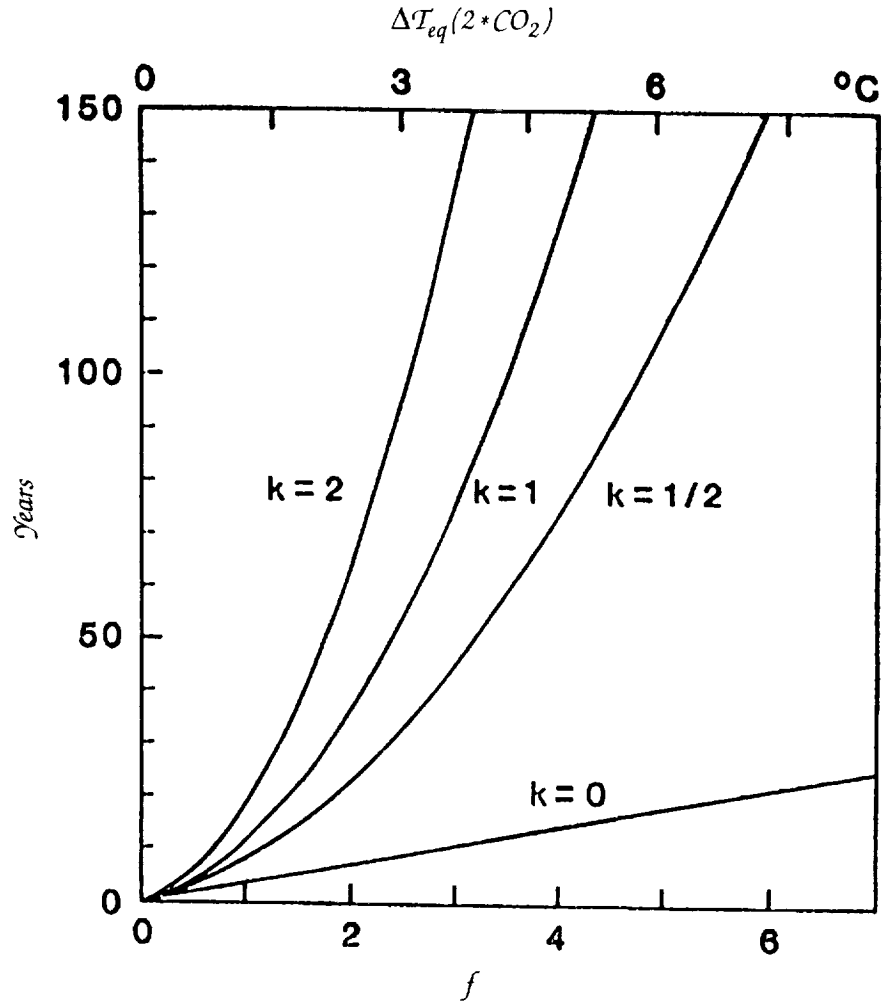
$$\Delta T_{eq}(2*CO_2)$$

Figure 7. Ocean surface response time (time to reach $1 - e^{-1}$ of equilibrium response) for a one-dimensional diffusive ocean model as a function of climate sensitivity to doubled CO_2 [ΔT_{eq} ($2*CO_2$)] or equivalently as a function of the climate feedback factor f. Mixed layer depth is 100 m and results for various vertical diffusion coefficients k (cm^2/s) are shown (adapted from Hansen et al., 1985; © 1985 by the AAAS).
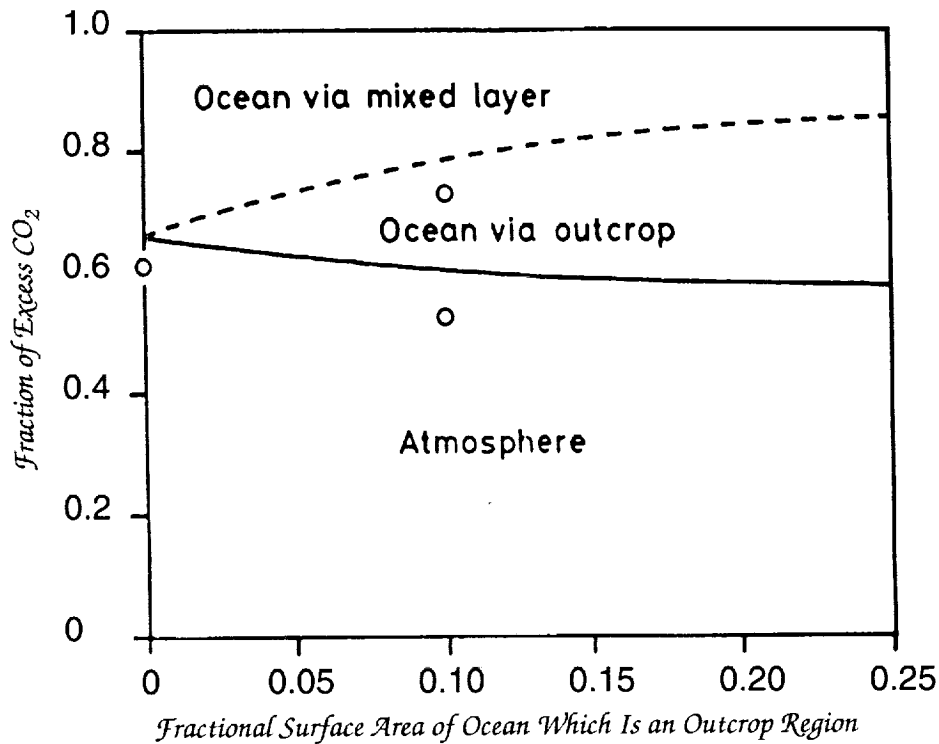
Figure 8. Fractions of the CO_2 added exponentially with an e-folding time of 22.5 years which are taken up by the ocean (diffusion into mixed layer plus simulated advection into deep water via an outcrop) as a function of the relative area of the outcrop. Circles denote fractions of bomb-produced ^{14}C taken up by the different media for relative outcrop areas of 0.0 and 0.1 (adapted from Siegenthaler, 1983).

posphere. As the water cools, it sinks, to be replaced by more warm water from the south (Broecker, 1987; Broecker and Denton, 1990). This northward flow of warm water in a "conveyor belt" keeps Europe warm during its winters. However, if sea ice invaded the North Atlantic and melted there, this would inhibit sinking (e.g., by the same mechanism in which the thermohaline circulation weakened due to increased river runoff and precipitation in the coupled ocean-atmosphere climate model of Stouffer et al., 1989). This would tend to decelerate the conveyor belt and cool Europe. This is just a hypothesis, but it could mean that one signal of greenhouse warming may actually be a cooling in some locations, which draws attention to the different results that could arise in a coupled ocean-atmosphere model but not in a model with prescribed sea surface temperatures or a horizontally static oceanic mixed layer. In fact, many ocean models that do have a circulation force the model to

observed climatology, which short-circuits many potential feedbacks when the climate is changing. We ultimately need realistic models that predict the changes in the ocean circulation as the climate changes and the resultant feedbacks to the climate and nutrient budgets (i.e., phytoplankton populations). The phytoplankton play a role in the uptake of CO_2 as well as the release of DMS, which, as discussed earlier, may be an important influence on the formation and radiative properties of clouds.

Land Surface Hydrology and Hydrology-Vegetation Coupling

The relationship between vegetation, soils, water flow, and weather patterns is complex and fundamental to life on the continents. The large-scale correlations between seasonal vegetation index, deep convective clouds (Warren et al., 1986), and surface albedo (Ramanathan et al., 1989) are quite evident. Vegetation is a major contributor to the absorption of sunlight over the land and, thus, to the local and global radiation budget. The albedo over vegetation is less than half that over bare land (Charney et al., 1975). Changing land vegetation cover can thus alter the net solar absorption. In addition, vegetation pumps water from soils into the atmosphere through evapotranspiration, thereby regulating the relative amounts of water in the atmosphere and in the soils. Thus, the vegetation affects the local and downstream water and latent heat budget. Shukla and Mintz (1982) illustrate the control vegetation could have on the regional climate. Figure 9 shows the significant effect soil moisture can have on precipitation patterns, with Figure 9a having a wet soil and Figure 9b having a dry soil boundary. Shukla and Mintz (1982) also show the effects of the soil moisture on surface temperature and pressure. The dry soil causes the land to be warmer and produces lower pressures because the energy from solar insolation cannot go into evaporation at the surface. Furthermore, there are fewer clouds (since there is less water to feed them), and therefore even more solar radiation reaches the surface. Thus vegetation is a major influence on regional climate.

On the other hand, vegetation is itself dependent on the climate. Different vegetation types thrive in different climates (Running and Coughlin, 1988; Clark, 1990, 1991). Some species are very sensitive to precipitation and solar input. Therefore, as these change, so will the vegetation. Furthermore, as regions become more dry the fire potential increases, and large areas of vegetation can potentially be cleared by burning. This can then influence what new vegetation will grow (Clark, 1990, 1991). Thus, changes in climate can both directly
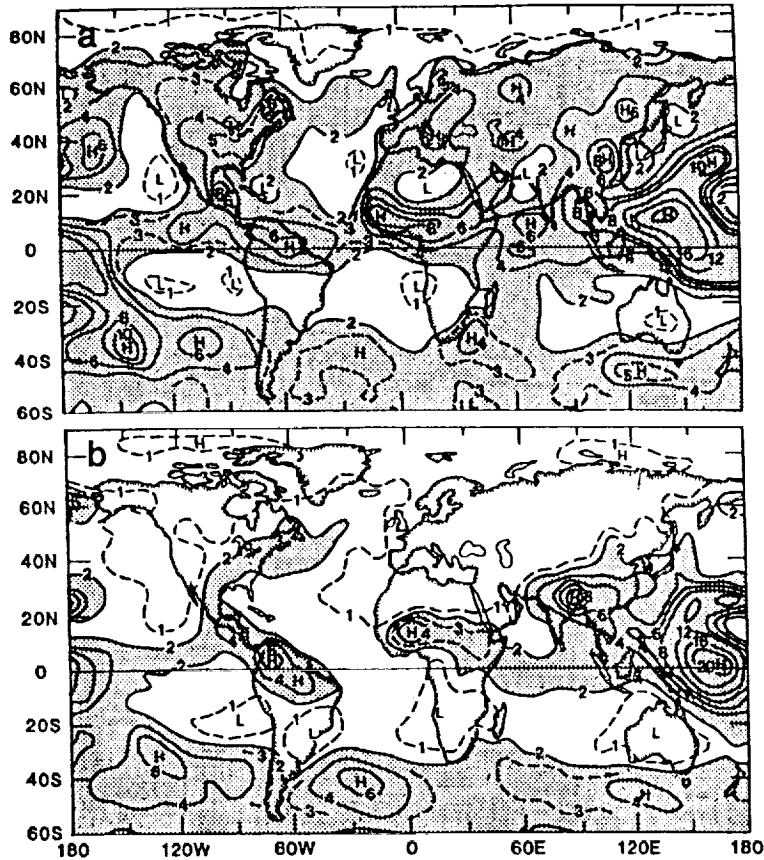
Figure 9. Model simulated July precipitation (mm/day) in (a) the wet soil and (b) the dry soil case (adapted from Shukla and Mintz, 1982; © 1982 by the AAAS).

and indirectly alter the vegetation. One feedback mechanism is illustrated in a well-known theory of desertification (Charney et al., 1975). Charney et al. (1975, 1977) show that as vegetation is cleared, the albedo increases, evapotranspiration decreases, subsidence occurs, and the normal precipitation is suppressed. Thus, this feedback dries out the surface, and recovery of the vegetation is severely inhibited. It is apparent, therefore, that accurate models for predicting future climate change cannot merely specify the vegetation at the surface, but instead must include vegetation as an internal variable.

For the current global GCMs, the effects of vegetation need to be parameterized since the scale of the relevant ecosystems is much smaller than that of a model grid box. These parameterizations must take account of local topography, water sources, and soil types since these are some of the crucial influences on vegetation cover. Various

simple vegetation/hydrology schemes in the GCMs of today give predictions that do not agree well with observations or with one another on a regional scale. Figure 10 shows the different predictions of soil moisture from several different GCMs. For these calculations, both the subgrid-scale convective and vegetation parameterizations contribute to the distinct differences.
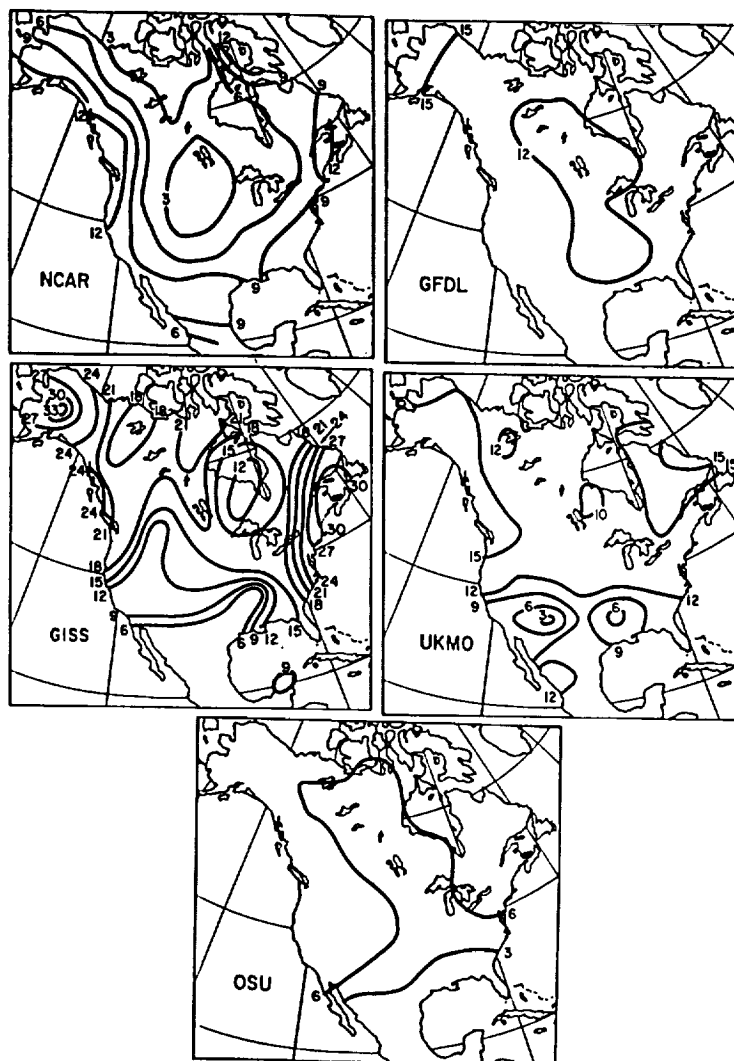

Figure 10. Present-day simulations of soil moisture in winter for North America obtained in general circulation climate models from the National Center for Atmospheric Research, Geophysical Fluid Dynamics Laboratory, Goddard Institute for Space Studies, U.K. Meteorological Office, and Oregon State University. Units are cm of water (adapted from Kellogg and Zhao, 1988).

Biogeochemistry of the Long-Lived Greenhouse Gases

Current concerns about future climate change are driven in large part by the undeniable observational evidence that several of the so-called long-lived greenhouse gases (CO_2, CH_4, N_2O, chlorofluorocarbons) are increasing presently at very significant rates. These increases, coupled with expected feedbacks increasing the concentration of the major greenhouse gas, the short-lived H_2O molecule, are predicted to lead to a significant warming over the next century (e.g., Dickinson and Cicerone, 1986). However, we lack the detailed biogeochemical and physical knowledge of individual sources and sinks for the long-lived greenhouse gases (with the exception of the chlorofluorocarbons) needed to explain quantitatively these present trends and to project them accurately into the future.

The long-lived greenhouse gases can be conveniently divided into three categories based on their chemical reactivity:

- *First category:* Some of the long-lived species are very inert (lifetimes exceeding 70 years) because they can be destroyed only by mixing up into the stratosphere above 25 kilometers altitude. Here, they can be dissociated by solar ultraviolet photons with wavelengths less than 250 nm. In this category are the industrial chlorofluorocarbons $CFCl_3$, CF_2Cl_2, and $CF_2ClCFCl_2$, which are widely used as refrigerants, propellants, plastic foaming agents, and solvents and which have lifetimes of around 45, 125, and 110 years respectively at the present time (Golombeck and Prinn, 1986, 1989, 1991, personal communication). Measurements made in the Atmospheric Lifetime Experiment/Global Atmospheric Gases Experiment (ALE/GAGE) network of automated stations (located in Ireland, Oregon, Barbados, Samoa, and Tasmania; Prinn, 1988; Prinn et al., 1983) indicate that $CFCl_3$, CF_2Cl_2, and $CF_2ClCFCl_2$ are currently increasing at rates of about 5%, 5%, and 10% per year respectively over the globe (Figure 11). Also in this class is N_2O, which has a present-day lifetime of about 130 years and is increasing at 0.2 to 0.3% per year (Figure 11) and has both natural (soils, ocean) and anthropogenic (disturbed and fertilized soil, combustion) sources. Analysis of ALE/GAGE N_2O data using inverse methods yields the conclusion that tropical sources of this gas compose 52–68% of the global total (Prinn et al., 1990). We need to understand these sources better and discern their sensitivity to climate changes. Another point worth noting is that all of the gases in this first category, when dissociated in the stratosphere, yield reactive species that catalytically destroy ozone, and some of them play a major role in the processes causing the Antarctic ozone hole. Destruction of
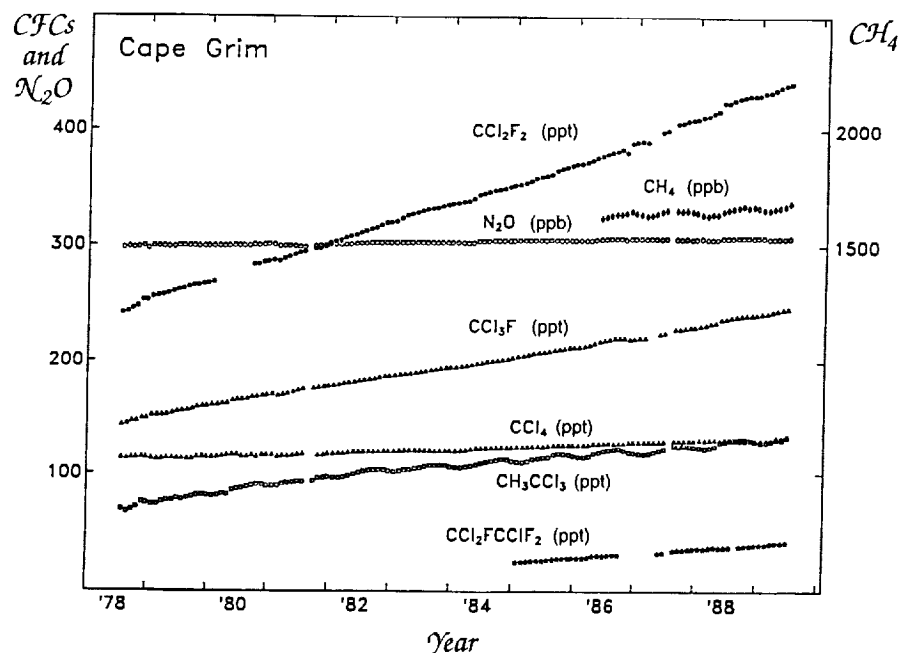
Figure 11. Monthly average concentrations of various long-lived trace gases measured at the Cape Grim, Tasmania, station of ALE/GAGE. Left vertical axis gives numerical values for mixing ratios of all compounds except CH_4, for which values are on the right vertical axis. Units are given on the data lines (from R. Prinn, P. Fraser, P. Simmonds, R. Rasmussen, F. Alyea, D. Cunnold, A. Crawford, and R. Rosen, personal communication).

stratospheric ozone in turn increases ultraviolet dosages at the surface, affecting living organisms and influencing the oxidation process in the lower atmosphere by accelerating photodissociation of O_3 to produce $O(^1D)$.

• *Second category:* Long-lived species in this category are less inert (lifetimes typically less than 15 years) because they can be destroyed by reaction with OH in the lower atmosphere. In this category is atmospheric CH_4 with a lifetime of 9.6 years (Prinn et al., 1987), which is increasing today at about 1% per year (Figure 11; see also Blake and Rowland, 1988). Methane (like N_2O) has both natural (wetlands, tundra) and human-controlled (cattle, combustion, rice agriculture) sources (Ehhalt, 1988; Cicerone and Oremland, 1988). Also in this category is the widely used industrial solvent and cleaning agent methyl chloroform (CH_3CCl_3) with a lifetime of 6.3 years (Prinn et al., 1987), which is increasing globally at about 4% per year (Figure 11). Finally, in this category are the hydrochlorofluorocarbons such as $CHClF_2$ (16-year present-day lifetime), currently increasing at about 10% per year, and

$CHCl_2CF_3$ (1.5 year steady-state lifetime), and CH_2FCF_3 (15-year steady-state lifetime), proposed as industrial replacements for the chlorofluorocarbons $CFCl_3$ and CF_2Cl_2.

As reviewed by Crutzen (1979), the concentrations of OH radicals are determined to a significant extent by short-lived species whose life cycles begin and end on local and regional scales (e.g., NO, NO_2, O_3, CO, hydrocarbons, etc., in Figure 12). Thus the global atmospheric chemistry of the long-lived species in the second category is linked in very important ways to the local and regional-scale atmospheric chemistry of the short-lived species that determine OH levels. One important implication of this linkage is that the positive trends in species like CH_4 may in part be
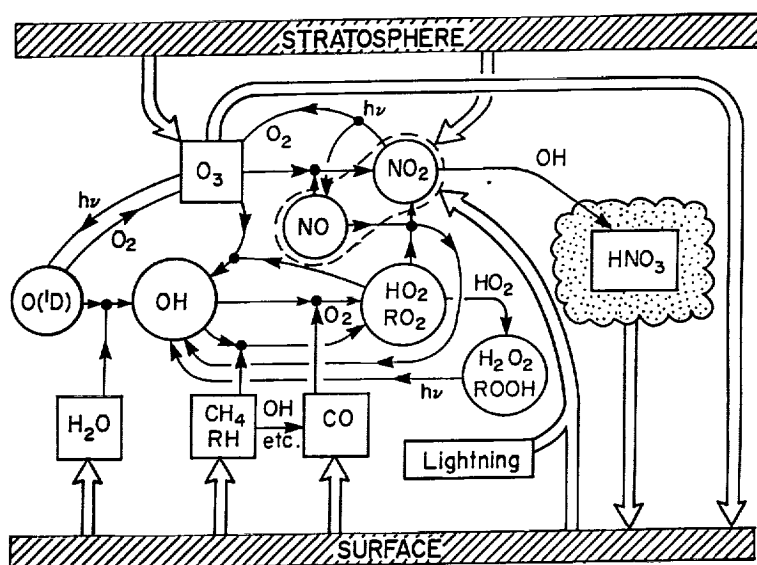

Figure 12. Schematic outlining the major recognized gas-phase chemistry in the troposphere. Black dots denote occurrence of chemical reactions. Thin arrows denote pathways for chemical reactions, while thick arrows denote fluxes of species from sources or to sinks. In continental air, rich in nitrogen oxides, NO is a major reactant for recycling HO_2 to OH and photodissociation of the resultant NO_2 is a major source for ozone. The dashed line enclosing NO and NO_2 signifies that both are produced from surface sources and lightning. In remote marine air, where nitrogen oxide levels are low, the major recycling of HO_2 to OH occurs through peroxide (H_2O_2, ROOH) formation and subsequent photodissociation. Reaction of HO_2 with O_3 provides another OH recycling mechanism in both environments. The OH and NO_2 are removed by formation of HNO_3, which is scavenged by clouds, indicated by the dotted area.

due to a decrease in OH radicals and thus a decrease in CH_4 loss rates rather than exclusively to an increase in CH_4 emission rates. Another implication is that the destruction of long-lived gases in this second category is weighted heavily to the hot tropical lower atmosphere whose local and regional chemistry we are only beginning to be informed about (Donahue and Prinn, 1990).

* *Third category:* CO_2 requires a category of its own. It is essentially chemically inert in the atmosphere and is cycled between atmosphere, upper ocean, green vegetation, and soils on decadal time scales and between the upper ocean and deep ocean on a time scale of a few hundred years. It is currently increasing at a rate of about 0.34% per year (Figure 13; Keeling, personal communication) and possesses a significant annual cycle driven by uptake of CO_2 by photosynthesizing vegetation in spring and summer and release of CO_2 by decaying vegetation in fall and winter. Classical ideas, as reviewed by Oeschger and Siegenthaler (1988), had the oceans playing the major role as a sink for carbon dioxide. A typical global budget has the current fossil fuel combustion source (5300 Tg C/yr) opposed by an oceanic sink (2300 Tg C/yr) to yield the observed atmospheric increase (3000 Tg C/yr). The land biosphere was generally considered to be a small contributor to the budget, although estimates of the deforestation source ranged from 400 to 2600 Tg C/yr. A recent comparison of the observed CO_2 latitudinal gradient with a global model containing only an ocean sink (Tans et al., 1990) showed poor agreement (Figure 14).
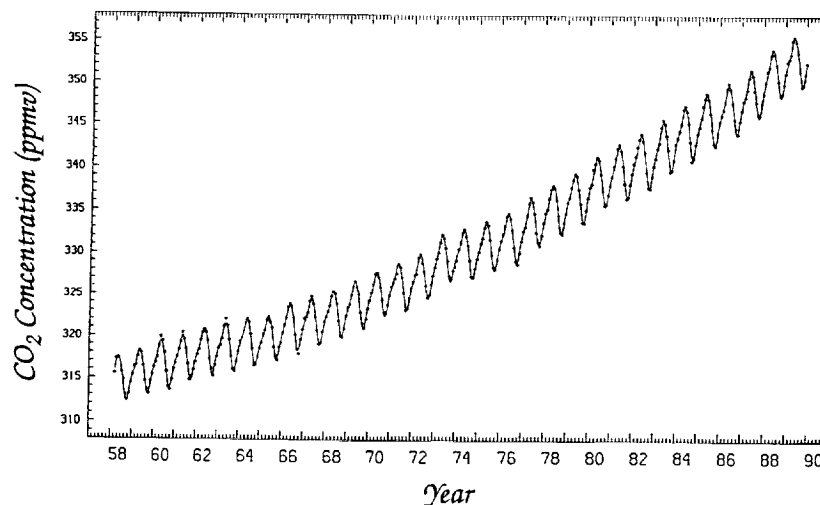

Figure 13. Concentration of CO_2 (ppmv) measured at Mauna Loa Observatory, Hawaii (C.D. Keeling, personal communication).
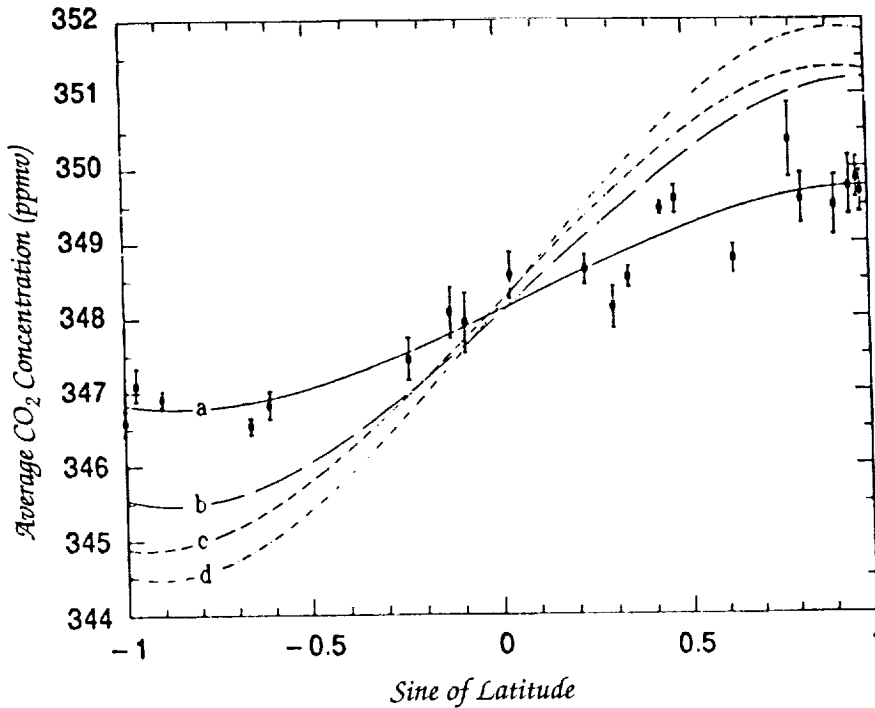
Figure 14. Observed CO_2 mixing ratios (circles with 1 sigma error bars), a cubic polynomial fit to observed CO_2 (line a), and predicted CO_2 in three GCM model runs (lines b, c, d). In the model runs the ocean is the only CO_2 sink, and this sink is computed in different ways in the three runs. A good fit (not shown) to the observations is obtained if a large Northern Hemisphere continental sink is included and the ocean sink decreased appropriately (adapted from Tans et al., 1990; © 1990 by the AAAS).

A new, significant Northern Hemispheric sink is needed to fit the data, but the available ocean uptake estimates do not allow the Northern Hemispheric oceans to provide this sink. Tans et al. concluded therefore that a significant Northern Hemispheric continental sink (about 2700 Tg C/yr) augmented by a smaller oceanic sink (about 1000 Tg C/yr) was needed to balance the atmospheric accumulation (3000 Tg C/yr), the fossil fuel input (5300 Tg C/yr), and the deforestation input (1400 Tg C/yr). Thus the ocean sink and the *net* biospheric sink (2700 –1400 = 1300 Tg C/yr) are comparable. If correct, this implies that continental forest regrowth and soil carbon uptake will need to be understood and appropriately modeled. Of particular interest is the possibility of CO_2 fertilization. Perhaps related to this is the increasing amplitude of the CO_2 annual cycle in recent years (Figure 13). It is worth noting, however, that the available $^{13}C/^{12}C$ data do not indicate a biospheric sink of the size needed here (Keeling et al., 1989).

Better knowledge of the controlling mechanisms and magnitudes of the individual sources and sinks for the greenhouse gases is essential for developing the needed models for reliable prediction of future emissions and for inclusion of potential feedbacks between these source and sink rates and climate change. Of particular importance is improved understanding of the role of the biota as trace gas sources and sinks and the effects of climate change on these sources and sinks (see, e.g., Prinn, 1992). The potential for such biogeochemical feedbacks is seen in the analyses of gases trapped in ice cores, which show this effect over the past 150,000 years where variations in concentrations of both methane and carbon dioxide are *correlated* with variations of temperature (Chappellaz et al., 1990). In particular, CH_4 and CO_2 are generally low during the ice ages and high during the warm interglacial epochs (Figure 15). This suggests the existence of a biogeochemical-climate feedback whereby increases in temperature or greenhouse gas concentrations lead to increases in greenhouse gas emissions or global warming respectively.

Upper Atmospheric Chemistry and Circulation

Changes in surface trace gas emissions, stratospheric-tropospheric exchange rates, and stratospheric temperatures and circulation will all affect the ozone layer. N_2O, methane, industrial chlorofluorocarbons like $CFCl_3$ and CF_2Cl_2, and water vapor are transported from the surface up into the stratosphere where photochemical reactions driven by solar ultraviolet radiation can decompose them to form a number of very reactive species (NO, NO_2, Cl, ClO, OH, HO_2) which can catalytically destroy ozone. Because stratospheric ozone is produced essentially exclusively by ultraviolet dissociation of O_2, its rate of global production is set externally by the supply of ultraviolet radiation from the sun. The global rate of destruction of ozone depends, however, on the supply of catalysts, which is rapidly rising due to continued chlorofluorocarbon emissions at the surface. Removal of the catalysts from the stratosphere occurs through their (partially reversible) conversion to harmless reservoir species (HNO_3, $ClONO_2$, HCl, etc.), many of which can be transported down again to the troposphere ultimately to rain out or deposit at the surface.

A dramatic illustration of the fact that the global chemical system is changing is provided by the Antarctic ozone hole phenomenon (Figure 16). This phenomenon can occur because temperatures in
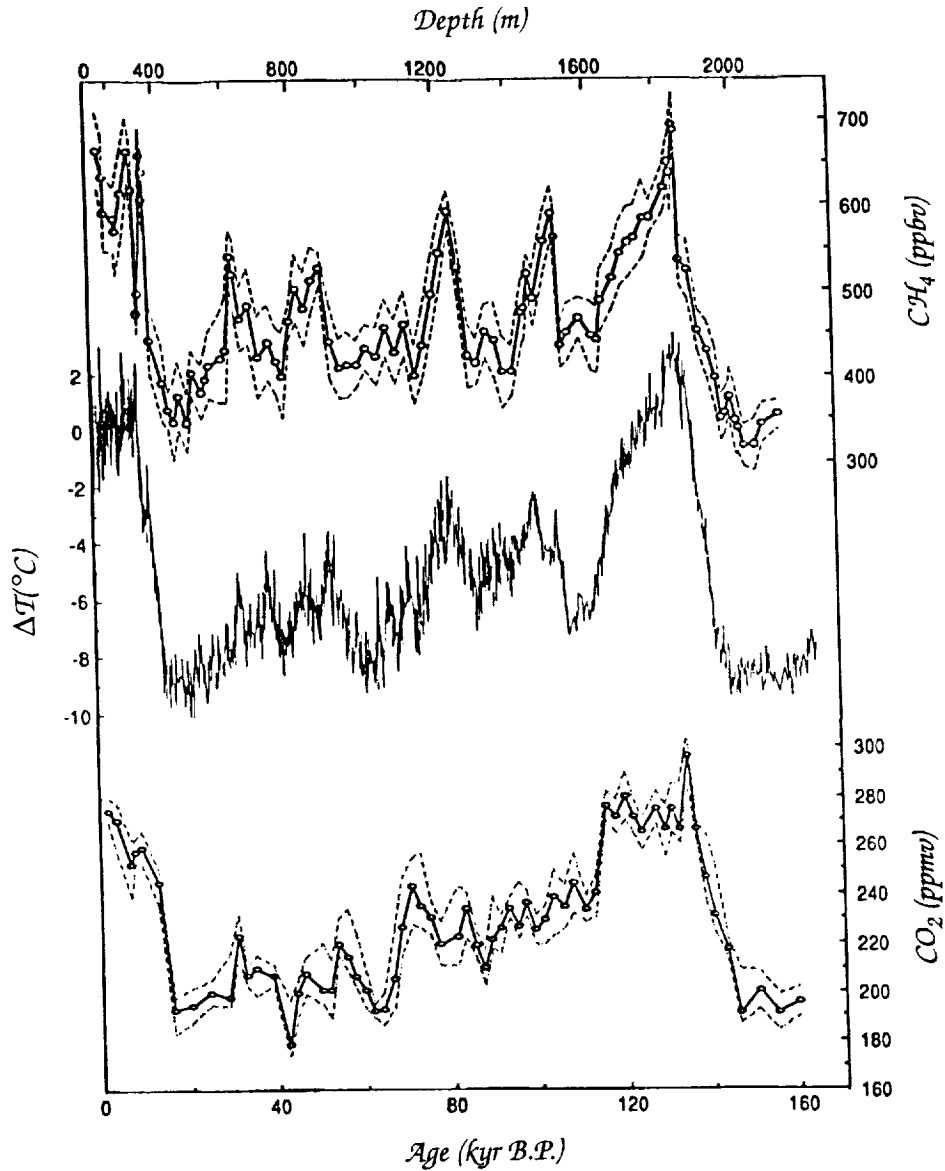
Figure 15. Vostok ice-core analyses of CH_4 (upper curves, 2 sigma errors), temperature relative to present as deduced from H_2O isotopes (middle curve), and CO_2 (lower curve, 2 sigma errors). Depth scale applies to CO_2 and CH_4. Due to downward diffusion the gases are younger than the ice in which they are trapped (adapted from Chappellaz et al., 1990; © 1990, Macmillan Magazines Ltd.).
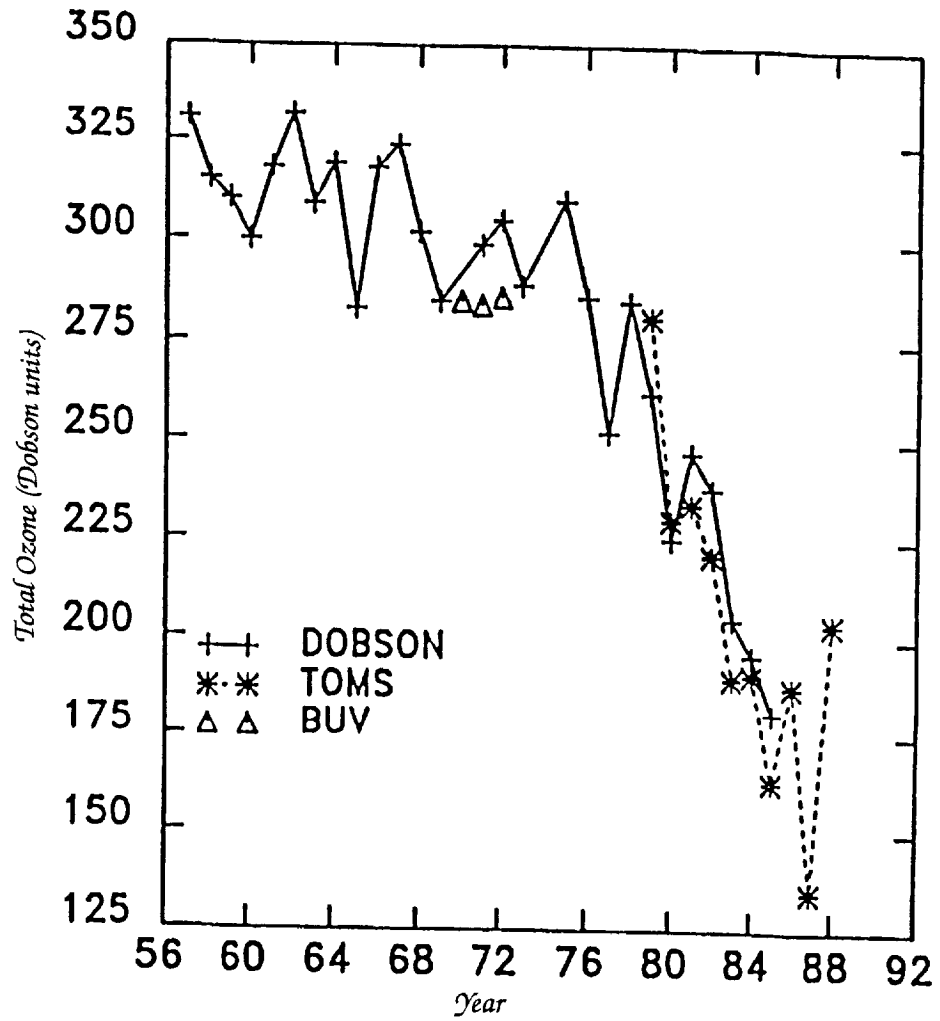
Figure 16. October monthly mean total ozone measurements over Halley Bay
as measured by Halley Bay Dobson and Nimbus 4 BUV (backscatter
ultraviolet) instruments. The polar minimum values for TOMS (total ozone
mapping spectrometer) for October are also shown. Dobson unit is 2.7×10^{16}
ozone molecule per cm^2 (Schoeberl et al., 1989; Stolarski, 1988).

ANTARCTIC OZONE HOLE

CHLORINE RELEASE

$$C\ell ONO_2 + HC\ell$$

$$\xrightarrow{\text{ice}} C\ell_2(gas) + HNO_3(ice)$$

$$C\ell_2(gas) \xrightarrow[\text{sunlight}]{\text{weak}} C\ell + C\ell$$

$$2(C\ell + O_3) \longrightarrow 2C\ell O + 2O_2$$

CATALYTIC CYCLE

$$2C\ell O \longrightarrow C\ell OOC\ell$$

$$C\ell OOC\ell \xrightarrow[\text{sunlight}]{\text{strong}} 2C\ell + O_2$$

$$2(C\ell + O_3) \longrightarrow 2(C\ell O + O_2)$$

$$2O_3 \longrightarrow 3O_2$$

S

$$u \lesssim 50-70\,m/sec$$

COLD ISOLATED AIR

10−50km

CIRCUMPOLAR VORTEX (JET)

45−75°S

POLAR STRATOSPHERIC
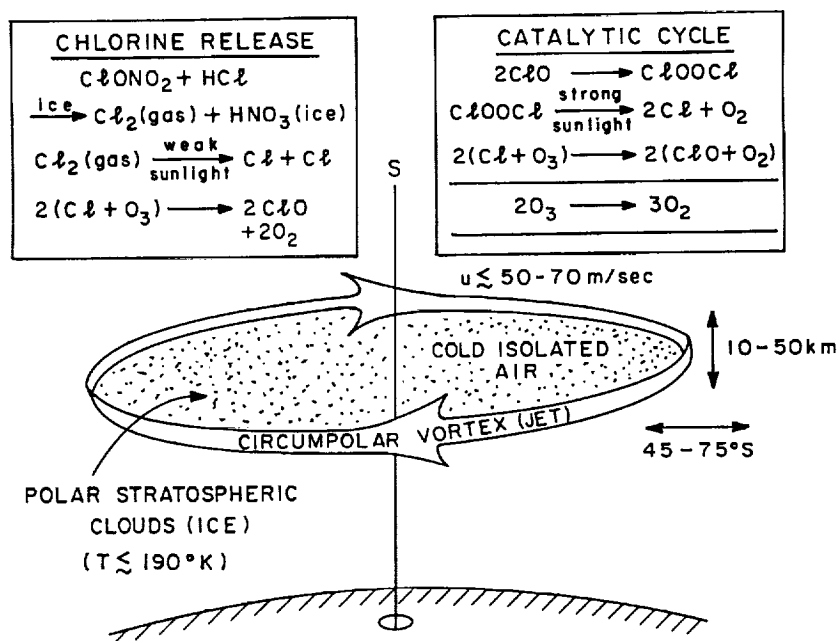CLOUDS (ICE)

$$(T \lesssim 190°K)$$

Figure 17. Schematic showing the vortex circulation, ice clouds, chlorine release reactions, and catalytic ozone destruction reactions involved in the Antarctic ozone hole.

the meteorologically isolated air mass lying between 10 and 30 km altitude in the Antarctic winter become so low (less than 190 K) that ice crystals condense in this region (Figure 17). Decomposition of some of the catalyst reservoir species occurs on and within these ice crystals, producing ClO in the early Antarctic spring. The ClO levels become very high because HNO_3 remains in the ice and is therefore not available to contribute to the conversion of ClO back to its relatively harmless reservoir compound $ClONO_2$. The scarcity in the Antarctic spring of ultraviolet radiation capable of decomposing O_3 means that different catalytic cycles operate here than the ones operating in tropical regions, which require O atoms produced by O_3 photodissociation (e.g., Rowland and Molina, 1975). The reaction sequence shown in Figure 17 serves to efficiently destroy O_3 without requiring O_3 photodissociation and without destroying ClO (Molina et al., 1987).

Theoretical models of the greenhouse effect indicate that a rise in the level of the greenhouse gases will tend not only to warm the earth's surface and lower atmosphere but also to *cool* the stratos-

phere, due to either the rise in a greenhouse gas, as is the case for CO_2, or the depletion of ozone, as in the case of rising chlorofluorocarbons (e.g., Ramanathan et al., 1985; Wang et al., 1991). This cooling of the stratosphere is expected to affect the ozone layer by decreasing ozone destruction in equatorial regions by slowing down the destruction reactions in these regions and increasing ozone destruction in the Antarctic (and also in the Arctic if cooling is sufficiently large) by increasing the extent of the polar ice clouds. These effects would be added to the increased ozone destruction expected due to the still rising chlorofluorocarbon concentrations. The stratospheric cooling by the greenhouse gases combined with these ozone layer changes will in turn affect the circulation at this level and conceivably at lower levels also. Also, changes in the intensity of tropical convection and midlatitude storms associated with a global warming are likely to alter significantly tropospheric-stratospheric exchange rates of trace gases involved in the ozone layer chemistry.

We therefore need realistic models of stratospheric circulation and chemistry that can be coupled with models of the lower atmosphere to improve the accuracy of tropospheric as well as stratospheric predictions.

Concluding Remarks

Understanding and modeling the above five fundamental processes provides a major interdisciplinary challenge with both observational and theoretical components. Several ongoing projects of the World Climate Research Program and the International Geosphere-Biosphere Program will all make large contributions. These projects include among others the International Global Atmospheric Chemistry (IGAC) project, Joint Global Ocean Flux Study (JGOFS), Global Energy and Water Cycle Experiment (GEWEX), Global Change and Terrestrial Ecosystems (GCTE) project, Tropical Oceans and Global Atmosphere (TOGA) project, and the World Ocean Circulation Experiment (WOCE). Later this decade the Earth Observing System (EOS) of the National Aeronautics and Space Administration will add a major satellite remote sensing capability relevant to many of these projects.

Acknowledgments

supported by the National Science Foundation and the National Aeronautics and Space Administration.

References

Bentley, C.R. 1984. Some aspects of the cryosphere and its role in climate change. In *Climate Processes and Climate Sensitivity* (J.E. Hansen and T. Takahashi, eds.), Geophysical Monograph 29, American Geophysical Union, Washington, D.C., 207–220.

Betts, A.K. 1986. A new convective adjustment scheme. Part I: Observational and theoretical basis. *Quarterly Journal of Research of the Meteorological Society 112*, 677–691.

Blake, D., and S. Rowland. 1988. Continuing world-wide increase in tropospheric methane, 1978 to 1987. *Science 239*, 1129–1131.

Broecker, W.S. 1987. Unpleasant surprises in the greenhouse? *Nature 328*, 123–126.

Broecker, W.S., and G.H. Denton. 1990. What drives the glacial cycles? *Scientific American 262*, 49–56.

Broecker, W.S., and T.H. Peng. 1982. *Tracers in the Sea.* Lamont-Doherty Geological Observatory, New York.

Carissimo, B.C., A.H. Oort, and T.H. Vonder Haar. 1985. Estimating the meridional energy transports in the atmosphere and ocean. *Journal of Physical Oceanography 15*, 82–91.

Chappellaz, J., J. Barnola, D. Raynand, Y. Korotkevich, and C. Lorius. 1990. Ice core record of atmospheric methane over the past 160,000 years. *Nature 345*, 127–131.

Charlson, R.J., J.E. Lovelock, M.O. Andreae, and S.G. Warren. 1987. Oceanic phytoplankton, atmospheric sulphur, cloud albedo and climate. *Nature 326*, 655–661.

Charney, J., P.H. Stone, and W.J. Quirk. 1975. Drought in the Sahara: A biogeophysical feedback mechanism. *Science 187*, 434–435.

Charney, J., W.J. Quirk, S. Chow, and J. Kornfield. 1977. A comparative study of effects of albedo changes on drought in semi-arid regions. *Journal of the Atmospheric Sciences 34*, 1366–1385.

Cicerone, R., and R. Oremland. 1988. Biogeochemical aspects of atmospheric methane. *Biogeochemical Cycles 2*, 299–327.

Clark, J.S. 1990. Fire and climate change during the last 750 years in north-western Minnesota. *Ecological Monographs 60(2)*, 135–139.

Clark, J.S. 1991. Ecosystem sensitivity to climate change and complex responses. In *Global Climate Change and Life on Earth* (R. Wyman, ed.), Chapman and Hall, New York.

Crutzen, P. 1979. The role of NO and NO_2 in the chemistry of the troposphere and stratosphere. *Annual Review of Earth and Planetary Science 7*, 443–472.

Dickerson, R.R., G.J. Huffman, W.T. Luke, L.J. Nunnermacker, K.E. Pickering, A.C.D. Leslie, C.G. Lindsey, W.G.N. Slinn, T.J. Kelly, P.H. Daum, A.C. Delaney, J.P. Greenberg, P.R. Zimmerman, J.F. Boatman, J.D. Ray, and D.H. Stedman. 1987. Thunderstorms: An important mechanism in the transport of air pollutants. *Science 235*, 460–465.

Dickinson, R., and R. Cicerone. 1986. Future global warming from atmospheric trace gases. *Nature 319*, 109–115.

Donahue, N., and R. Prinn. 1990. Non-methane hydrocarbon chemistry in the remote marine boundary layer. *Journal of Geophysical Research 95*, 18387–18411.

Ehhalt, D.H. 1988. How has the atmospheric concentration of CH_4 changed? In *The Changing Atmosphere* (F. Rowland and I. Isaksen, eds.), John Wiley and Sons, Chichester, England, 25–32.

Emanuel, K.A. 1990. *A Scheme for Representing Cumulus Convection in Large-Scale Models*. Report No. 3, Center for Global Change Science, Massachusetts Institute of Technology, Cambridge.

Golombeck, A., and R. Prinn. 1986. A global three-dimensional model of the circulation and chemistry of $CFCl_3$, CF_2Cl_2, CH_3CCl_3, CCl_4, and N_2O. *Journal of Geophysical Research 91*, 3985–4001.

Golombeck, A., and R. Prinn. 1989. Global 3-dimensional model calculations of the budgets and present-day atmospheric lifetimes of $CF_2ClCFCl_2$ and $CHClF_2$. *Geophysical Research Letters 16*, 1153–1156.

Hansen, J., G. Russel, A. Lacis, I. Fung, D. Rind, and P. Stone. 1985. Climate response times: Dependence on climate sensitivity and ocean modelling. *Science 229*, 857–859.

Hibler, W.D. 1990. *Sea Ice Response to Global Climate Change*. Review Document for Brookhaven Workshop on Global Climate Feedbacks.

Keeling, C.D., S.C. Piper, and M. Heimann. 1989. A three dimensional model of atmospheric CO_2 transport based on observed winds: 4. Mean annual gradients and interannual variations. In *Aspects of Climate Variability in the Pacific and the Western Americas* (D.H. Peterson, ed.), Geophysical Monograph 55, American Geophysical Union, Washington, D.C., 305–363.

Kellogg, W.W., and Z.-C. Zhao. 1988. Sensitivity of soil moisture to doubling of carbon dioxide in climate model experiments. Part I: North America. *Journal of Climate 1*, 348–366.

Kiehl, J.T., and V. Ramanathan. 1990. Comparison of cloud forcing derived from the Earth Radiation Budget Experiment with that simulated by the NCAR Community Climate Model. *Journal of Geophysical Research 95*, 11679–11698.

Kuo, H.L. 1974. Further studies of the parameterization of the influence of cumulus convection on large-scale flow. *Journal of the Atmospheric Sciences 31*, 1232–1240.

Manabe, S., J. Smagorinsky, and R.F. Strickler. 1965. Simulated climatology of a general circulation model with a hydrologic cycle. *Monthly Weather Review 93*, 769–798.

Molina, M., T. Tso, L. Molina, and F. Wang. 1987. Antarctic stratospheric chemistry of chlorine nitrate, hydrogen chloride, and ice: Release of active chlorine. *Science 238*, 1253–1257.

Newell, R.E. J.W. Kidson, D.G. Vincent, and G.J. Boer. 1972. *The General Circulation of the Tropical Atmosphere* (Vol. 1). MIT Press, Cambridge, Massachusetts, 258 pp.

Oeschger, H., and U. Siegenthaler. 1988. How has the atmospheric concentration of CO_2 changed? In *The Changing Atmosphere* (F. Rowland and I. Isaksen, eds.), John Wiley and Sons, Chichester, England, 5–23.

Oort, A.H., and T.H. Vonder Haar. 1976. On the observed annual cycle in the ocean-atmosphere heat balance over the Northern Hemisphere. *Journal of Physical Oceanography 6*, 781–800.

Philander, G.S., and E.M. Rasmusson. 1985. The Southern Oscillation and El Niño. *Advances in Geophysics 28A*, 197–215.

Prinn, R. 1988. How have the atmospheric concentrations of the halocarbons changed? In *The Changing Atmosphere* (F. Rowland and I. Isaksen, eds.), John Wiley and Sons, Chichester, England, 33–48.

Prinn, R. 1992. Cyclic closure of biogeochemical cycles: Vernadsky Loops. In *Trace Gases and the Biosphere* (B. Moore and D. Schimel, eds.), Global Change Institute Volume 1, UCAR/Office for Interdisciplinary Earth Studies, Boulder, Colorado, 79–86.

Prinn, R., P. Simmonds, R. Rasmussen, R. Rosen, F. Alyea, C. Cardelino, A. Crawford, D. Cunnold, P. Fraser, and J. Lovelock. 1983. The Atmospheric Lifetime Experiment, I: Introduction, instrumentation and overview. *Journal of Geophysical Research 88*, 8353–8368.

Prinn, R., D. Cunnold, R. Rasmussen, P. Simmonds, F. Alyea, A. Crawford, P. Fraser, and R. Rosen. 1987. Atmospheric trends in methyl chloroform and the global average for the hydroxyl radical. *Science 238*, 945–950.

Prinn, R., D. Cunnold, R. Rasmussen, P. Simmonds, F. Alyea, A. Crawford, P. Fraser, and R. Rosen. 1990. Atmospheric trends and emissions of nitrous oxide deduced from ten years of ALE/GAGE data. *Journal of Geophysical Research 95*, 18369–18385.

Ramanathan, V. 1981. The role of ocean-atmosphere interaction in the CO_2 climate problem. *Journal of the Atmospheric Sciences 38*, 918–930.

Ramanathan, V., and W. Collins. 1991. Thermodynamic regulation of ocean warming by cirrus clouds deduced from observations of the 1987 El Niño. *Nature 351*, 27–32.

Ramanathan, V., R. Cicerone, H. Singh, and J. Kiehl. 1985. Trace gas trends and their potential role in climate change. *Journal of Geophysical Research 90*, 5547–5566.

Ramanathan, V., R.D. Cess, E.F. Harrison, P. Minnis, B.R. Barkstrom, E. Ahmad, and D. Hartmann. 1989. Cloud-radiative forcing and climate: Results from the Earth Radiation Budget Experiment. *Science 243*, 57–63.

Rowland, F., and M. Molina. 1975. Chlorofluoromethanes in the environment. *Reviews of Geophysics and Space Physics 13*, 1–35.

Running, S.W., and J.C. Coughlan. 1988. A general model of forest ecosystem processes for regional applications. I. Hydrologic balance, canopy gas exchange and primary production processes. *Ecological Modelling 42*, 125–154.

Schoeberl, M., R. Stolarski, and A. Krueger. 1989. The 1988 Antarctic ozone depletion: Comparison with previous year depletions. *Geophysical Research Letters 16*, 377–380.

Shukla, J., and Y. Mintz. 1982. Influence of land-surface evapotranspiration on the Earth's climate. *Science 215*, 1498–1501.

Siegenthaler, U. 1983. Uptake of excess CO_2 by an outcrop-diffusion model of the ocean. *Journal of Geophysical Research 88*, 3599–3608.

Somerville, R.C.J., and L.A. Remer. 1984. Cloud optical thickness feedbacks in the CO_2 climate problem. *Journal of Geophysical Research 89*, 9668–9672.

Stolarski, R. 1988. Changes in ozone over the Antarctic. In *The Changing Atmosphere* (F. Rowland and I. Isaksen, eds.), John Wiley and Sons, Chichester, England, 105–119.

Stouffer, R., S. Manabe, and K. Bryan. 1989. Interhemispheric asymmetry in climate response to a gradual increase of atmospheric CO_2. *Nature 342*, 660–662.

Tans, P., I. Fung, and T. Takahashi. 1990. Observational constraints on the global atmospheric CO_2 budget. *Science 247*, 1431–1438.

Trenberth, K.E. 1979. Mean annual poleward energy transports by the oceans in the Southern Hemisphere. *Dynamics of the Atmosphere and Oceans 4*, 57–64.

Twomey, S. 1977. *Atmospheric Aerosols.* Elsevier, Amsterdam.

Wang, W.-C., M. Dudek, X.-Z. Liang, and J. Kiehl. 1991. Inadequacy of effective CO_2 as a proxy in simulating the greenhouse effect of other radiatively active gases. *Nature 350*, 573–577.

Warren, S., C. Hahn, J. London, R. Chervin, and R. Jenne. 1986. *Global Distribution of Total Cloud Cover and Cloud Type over Land.* Technical Note TN-273+STR, National Center for Atmospheric Research, Boulder, Colorado.